

# **Modeling of Negative Ion Transport in Cesium-Seeded Volume Negative Ion Sources**

Osamu Fukumasa and Ryo Nishida

*Department of Electrical and Electronic Engineering, Faculty of Engineering,  
Yamaguchi University, Tokiwadai 2-16-1, Ube 755-8611, Japan*

**Abstract.** Trajectories of  $H^-$  ions are calculated numerically by solving the 3D motion equation, including effects of collisional destruction, elastic collisions and charge exchange collisions. According to these trajectories, extraction probability of  $H^-$  ions produced at any location inside the source and energy of extracted  $H^-$  ions are discussed as a function of gas pressure. Effects of production zone and filter magnetic field on extraction probability are also discussed. The probability for surface produced  $H^-$  ions keeps nearly the constant value, and that for volume produced  $H^-$  ions decreases with gas pressure. The kinetic energy of extracted  $H^-$  ions is reduced mainly by charge exchange collision.

We also discuss the characteristics of extracted negative ion current combining the present numerical results and the results of the model calculation with the zero-dimensional code.

## 1. Introduction

Negative ion based neutral beam injection is one of the most promising candidates for heating and current drive of fusion plasma. By seeding a small amount of cesium (Cs) vapor into the volume ion source,  $H^-$  production has been increased by a factor of 2-4 and optimum pressure decreases to 0.8-1.0 Pa [1]. Although Cs effects have been observed by many researchers, the mechanism remains to be discussed. We have studied source modeling [2-6] and Cs effects on enhancement of  $H^-$  production in a tandem two-chamber system, i.e. the source and the extraction regions. According to our numerical results, it is confirmed that the dominant process for enhancement of  $H^-$  production is surface production [5, 6].

For discussing the pressure dependence of extracted  $H^-$  current, we have also estimated the extracted  $H^-$  ions, by taking into account stripping loss in the acceleration grid region only [4, 5]. But some  $H^-$  ions produced in the source aren't extracted because of collisional destructions. So, it is important to study the behavior of  $H^-$  ions in the second chamber, i.e. in the extraction region [7]. In addition, it has been reported that the beam divergence of surface produced  $H^-$  ions are nearly the same one as that of volume produced  $H^-$  ions [8]. However, the physical reason has not yet been clarified.

In this paper, we will discuss the extraction probability of  $H^-$  ions by using both model calculation [5] and  $H^-$  ion transport in the second chamber [7]. The preliminary results have been presented earlier [9, 10], herewith  $H^-$  ion transport and extracted  $H^-$  ions are further studied including effects of production zone and filter magnetic field. To clarify good beam optics of surface produced  $H^-$  ions, we will also study both mean kinetic energy and the velocity distribution of extracted  $H^-$  ions.

## 2. Simulation model and procedure

To simulate  $H^-$  production in a tandem two chamber system, we have used the zero-dimensional code with source model, shown in Fig. 1 [3-5]. In the present study, with using a coordinate system shown in Fig. 1 and 2, negative ion trajectory in the second chamber is calculated numerically, with width  $L = 30$  cm. Magnetic filter is set at 2 cm ( $= L_2$ ) upstream from a plasma grid (PG). The spatial profile of magnetic filter is given by the Gaussian profile  $B_y(y, z) = B_0 \exp[-(z-z_0)^2/l_B^2]$ , where  $z_0 = 2$  cm,  $l_B = 4$  cm and  $B_0 = 120$  Gauss. Surface confinement magnets field is also present. Sixteen columns of permanent magnets are arranged to construct line cusp field.

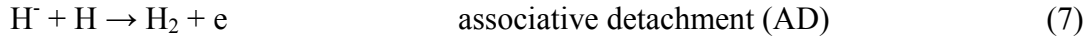
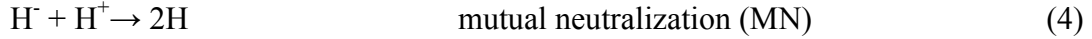
When a negative ion is produced, it moves inside the source until destruction or extraction. Trajectories of  $H^-$  ions are calculated numerically by solving the 3D motion equation as follows:

$$Mdv/dt = q(\mathbf{v} \times \mathbf{B}) + \mathbf{F}_{col}, \quad (1)$$

where  $M$  is mass of the  $H^-$  ion,  $q$  is charge,  $\mathbf{v}$  is the velocity vector and  $\mathbf{B}$  is the vector of magnetic field. The electric field is neglected in the above equation because it is negligibly small in the plasma region as compared with the electric field in the sheaths near the plasma grid and chamber walls. The second term on the right-hand side  $\mathbf{F}_{col}$  is the collision term, which is explained below. When  $\mathbf{x}$  is the vector of the position, the definition of velocity vector can be described as

$$d\mathbf{x}/dt = \mathbf{v}. \quad (2)$$

We solved equations (1) and (2) in three dimensions using the Runge-Kutta-Gill method as the initial value problem. The collisions between  $H^-$  ions and other particles are calculated by the Monte Carlo method [7, 11]. The following destruction, charge exchange and elastic collisions are taken into account:



Volume produced  $H^-$  ions are launched isotropically in all directions with an initial energy of 0.5 eV at any  $x, y$  location, except that axial points ( $z$  direction), where four launching points (i.e.  $z = 0.25, 0.75, 1.25$  and  $1.75$  cm), were used. The surface produced  $H^-$  ions are launched from the PG with an initial energy of 0.5, 1 and 2 eV due to potential difference between plasma potential and plasma grid potential. When  $H^-$  ions have reached the PG or destroyed by collisional processes, the calculation is finished.

The background plasma profiles are assumed to be uniform, and these values are obtained by the previous model calculation [4, 5] and are used to estimate mean free paths for collisions mentioned above. To determine the electron density dependence of  $H^-$  production and particle densities, calculation is performed as a function of electron density  $n_e(1)$  in the

first chamber on the assumption that other plasma parameters are kept constant [3-5]. A typical numerical result is summarized in Table 1. Plasma conditions for model calculation is as follows: the gas pressure  $p = 5$  mTorr, the electron density ratio between two chambers  $n_e(2)/n_e(1) = 0.2$ , density of  $e_f$  in the first chamber  $n_{fe}(1)/n_e(1) = 0.05$ , electron temperature in the first and second chambers are, respectively,  $\kappa T_e(1) = 5$  eV,  $\kappa T_e(2) = 1$  eV, and magnetic filter position  $L_1 : L_2 = 28 : 2$  cm (i.e.  $z_0 = L_2 = 2$  cm).

### 3. Numerical results and discussion

#### 3.1 Extraction probability and energy relaxation of negative ions

The trajectories of  $H^-$  ions are obtained by solving the 3D motion equation until ions are destroyed or extracted (i.e., reached to the PG). Typical orbits of  $H^-$  ions in the second chamber of the negative ion source are shown in Fig. 3.

At first, characteristic features of  $H^-$  ion trajectories (i.e. properties on  $H^-$  ion extraction) are discussed. To this end, for a certain plasma conditions, a set of five calculations (one calculation for surface produced  $H^-$  ions and four calculations for volume produced  $H^-$  ions with different four  $z$  positions) is done. We used  $10^3$  test  $H^-$  ions for one calculation. Table 2 shows the simulation result, where gas pressure is 5 mTorr. In the present case, 710 surface produced  $H^-$  ions reached the PG and extraction probability is about 28.4 % (geometrical transparency of the PG is assumed to be 40 %). For volume produced  $H^-$  ions, the probability to reach the PG depends strongly on the upstream distance  $z$  from the PG. Then, mean value of the extraction probability is about 5.2 %.

This probability depends on gas pressure. Table 3 shows another example of the simulation result, where gas pressure is 1 mTorr. According to the results in Tables 2 and 3, extraction probability of volume produced  $H^-$  ions slightly decreases with gas pressure. These characteristic features are clearly shown in Fig. 4. Effect of magnetic filter field on  $H^-$  trajectories is also discussed. Numerical result is shown in Fig. 5, where gas pressure is 5 mTorr, and  $B_0 = 120$  Gauss for two different  $l_B$ , i.e. 1 cm and 4 cm. There is scarcely difference in extraction probability due to difference of filter field.

$H^-$  ion transport (i.e. the extraction probability) depends on gas pressure. Discussing this point, the same calculations described above are done by changing gas pressure. In the present calculation, initial positions (i.e. birth points) of surface produced  $H^-$  ions are distributed at any location on the PG and those of volume produced  $H^-$  ions are also distributed at any location in the second chamber, i.e. three dimensional. Now,  $10^3$  test particles for surface produced  $H^-$  ions and  $2 \times 10^3$  test particles for volume produced  $H^-$  ions

are used, respectively. Numerical results are shown in Fig. 6. Extraction probability of volume produced  $H^-$  ions decreases with gas pressure nearly the same manner as that of surface produced  $H^-$  ions. It is remarkable, however, that extraction probability of surface produced  $H^-$  ions is much higher than that of volume produced  $H^-$  ions. Physical meaning is as follows: With increasing gas pressure, particle densities increase and mean free path of  $H^-$  ions decreases in its value. Therefore, transport of  $H^-$  ions in the extraction region decreases due to collisional effects. In particular, surface produced  $H^-$  ions injected into plasmas are reflected easily by elastic and charge exchange collisions and reach the PG. On the other hand, volume produced  $H^-$  ions are impeded to reach the PG by collisional processes.

Kinetic energy (KE) of  $H^-$  ions are reduced by elastic [13] and charge exchange [7] collisions. According to the Table 2, for surface produced  $H^-$  ions with initial energy 1eV, KE of extracted  $H^-$  ions is reduced to 0.66 eV. On the other hand, for volume produced  $H^-$  ions with 0.5 eV, KE of extracted  $H^-$  ions is reduced to 0.45 eV, and lower than that of surface produced  $H^-$  ions due to difference in initial energy of  $H^-$  ions. Although there is some difference between the velocity distribution of extracted  $H^-$  ions for surface produced  $H^-$  ions and that for volume produced  $H^-$  ions (not shown here), energy relaxation mentioned above and velocity distribution are the cause for good beam optics of negative ion current with Cs seeding [8]. As is shown in Table 2, in high-pressure case, charge exchange collision is the most dominant collision process. With decreasing  $p$  (see Table 3), however, effects of elastic collisions become remarkable. Therefore, both elastic collision and charge exchange collision play important roles in energy relaxation of the extracted  $H^-$  ions.

### 3.2 Estimation of extracted negative ion currents

Next, we will discuss pressure dependence of the extracted  $H^-$  current. Figure 7 shows the  $H^-$  densities,  $H^-(2)$ , in the second chamber obtained by the model calculation [3-5] as a function of  $p$  for  $n_e(1) = 5 \times 10^{12} \text{ cm}^{-3}$ . In this calculation, surface productions of  $H^-$  ions and  $H_2(v'')$  from H and positive ions are included. Details on wall conditions are reported elsewhere [5]. For no Cs case,  $H^-$  ions are produced by the so-called two-step pure volume process. With Cs, however,  $H^-(2)$  increases markedly due to surface production of  $H^-$  ions from H and positive ions [4, 5].

In order to discuss pressure dependence of the extracted  $H^-$  current [4, 5], previously, we estimated the extracted  $H^-$  ions from  $H^-(2)$  by taking into account only stripping loss of  $H^-$  ions in the extraction and acceleration grids region (see Fig.1). According to gas pressure distribution along the beam axis estimated by the Monte Carlo simulation [14], we calculate the survival factor  $F$  against the stripping loss of  $H^-$  ions, i.e.,  $H^- + H_2 \rightarrow H + H_2 + e$  and  $H^- +$

$H \rightarrow 2H + e$ .  $F$  is a decreasing function of pressure. Then, the extracted  $H^-$  ions, corresponding to the results in Fig. 7, are estimated by the product of  $H^-$  (2) in Fig. 7 with  $F$ . Namely, it is assumed that all of  $H^-$  ions in the second chamber are extracted. As is discussed in section 3.1, only a part of  $H^-$  ions in the second chamber can be extracted. So, the previous values of extracted  $H^-$  ions are overestimated.

Now, we will discuss and estimate the extracted  $H^-$  ions more precisely, with applying the results in section 3.1, from the results in Fig. 7. The procedure is as follows: At first,  $H^-$  (2) density is divided into two parts, i.e. surface produced  $H^-$  ions and volume produced  $H^-$  ions, by using the rates of surface production and volume production in the rate equation for  $H^-$  (2). Next, according to the extraction probabilities for both surface and volume produced  $H^-$  ions,  $H^-$  ions which can reach the plasma grid are estimated from the product of  $H^-$  ion densities of two types with the extraction probabilities, respectively. Then, total  $H^-$  ions are obtained by summing up those two parts. Finally, the extracted  $H^-$  ions are determined by the product of the above mentioned total  $H^-$  ions with survival factor  $F$ . This procedure is summarized in Table 4.

Figure 8 shows the extracted  $H^-$  ions with Cs, corresponding to the result in Fig. 7, as a function of  $p$ . Solid line is the previous result [4, 5], and solid points are the present estimated values. These values are much lower than the previous ones. The same procedure is also applied to  $H^-$  ions with pure volume production in Fig 7. These results, i.e. the extracted  $H^-$  ions with and without Cs, are shown in Fig. 9. In both case, the optimum pressure giving the highest  $H^-$  currents is observed clearly. With Cs injection, the extracted  $H^-$  current increases by many time compared with the current in pure volume case.

So far, we present only one example concerning the extraction of  $H^-$  current. To discuss pressure dependence of extracted  $H^-$  current, more numerical results for different  $n_e(1)$  should be required [5]. At any rate, extraction probability depends strongly on upstream distance from the PG (i.e. the extraction grid). Then, to increase the extracted negative ion currents, production of negative ions near the extraction grid should be enhanced much more.

## 4. Conclusions

The probability for  $H^-$  ions to reach the plasma grid (i.e. extraction probability) is estimated. As a whole, extraction probability is relatively low. It is confirmed that extraction probability for surface produced  $H^-$  ions is much higher than that for volume produced  $H^-$  ions. Within the present numerical conditions, the extraction probability for surface produced  $H^-$  ions keeps relatively high value (i.e. 24-30 %), and that for volume

produced  $H^-$  ions decreases in its value from 8 % to 3 % with increasing gas pressure. The kinetic energy of the extracted  $H^-$  ions is reduced by both charge exchange collisions with H and elastic collisions with  $H^+$ . There is a certain energy difference in extracted  $H^-$  ions between volume produced  $H^-$  ions and surface produced  $H^-$  ions. We have also discussed briefly the characteristics of extracted negative ion current with the use of both the present numerical results for extraction probability and the results of our previous model calculation.

## **Acknowledgements**

The authors would like to thank Prof. H. Naitou and S. Mori for their discussion and support in preparation of the present paper. A part of this work was supported by the Grant-in-Aid for Scientific Research from the Ministry of Education, Culture, Sports, Science and Technology, Japan. This work was also performed with the support of the NIFS LHD Project Research Collaboration.

## References

- [1] Okumura, Y. et al., Rev. Sci. Instrum. **63** (1992) 2708.
- [2] Fukumasa, O., J. Phys. **D22** (1989) 1668.
- [3] Fukumasa, O., J. Appl. Phys. **71** (1992) 3193.
- [4] Fukumasa, O. and Monji, H., Rev. Sci. Instrum. **71** (2000) 1234.
- [5] Fukumasa, O., IEEE T. Plasma Sci. **28** (2000) 1009.
- [6] Fujioka, T., Fukuchi, T. and Fukumasa, O., *Proceedings of the 25th International Conference on Phenomena in Ionized Gases* **2** (2001) 245.
- [7] Riz, D. and Pamela, J., Rev. Sci. Instrum. **69** (1998) 914.
- [8] Miyamoto, K. et al., *Proceedings of the 18th Symposium on Fusion Technology* **1** (1995) 625.
- [9] Fukumasa, O., Fukuchi, T. and Fujioka, T., *Proceedings of the 9th International Symposium on the Production and Neutralization of Negative Ions and Beams* (2002) 75.
- [10] Fukumasa, O. and Nishida, R., *Proceedings of the 10th International Symposium on the Production and Neutralization of Negative Ions and Beams* (2004) 159.
- [11] Ido, S., Hasebe, H. and Fujita, Y., Jpn. J. Appl. Phys. **32** (1993) 4761.
- [12] Hummer, D. G., Stebbings, R. F., Fite, W. L. and Branscomb, L. M., Phys. Rev. **119** (1960) 668.
- [13] Makino, K., Sakurabayashi, T., Hatayama, A., Miyamoto, K. and Ogasawara, M., Rev. Sci. Instrum. **73** (2002) 1051.
- [14] Takeiri, Y., Ando, A., Kaneko, O., Oka, Y., Tsumori, K., Akiyama, R., Asano, E., Kawamoto, T., Kuroda, T. and Kawakami, H., Rev. Sci. Instrum. **66** (1995) 2541.

## Figure captions

**Figure 1.** Simulation model for the tandem two-chamber system.

**Figure 2.** Model geometry of the second chamber used for the tandem system shown in Fig.1.

**Figure 3.** Examples of  $H^-$  ion trajectories in the second chamber : (a) a surface produced  $H^-$  ion (initial energy : 1 eV, birth point  $(x, y, z) = (0, 0, 0)$ ), (b) a volume produced  $H^-$  ion (initial energy : 0.5 eV, birth point  $(x, y, z) = (0, 0, 1.75 \text{ cm})$ ) .

**Figure 4.** Extraction probability as a function of  $z$ . Parameter is hydrogen gas pressure, where  $B_0 = 120 \text{ G}$  and  $l_B = 4 \text{ cm}$ .

**Figure 5.** Extraction probability as a function of  $z$ . Parameter is magnetic filter field, where gas pressure  $p = 5 \text{ mTorr}$ .

**Figure 6.** Pressure dependence of extraction probability for  $H^-$  ions: ● for surface produced  $H^-$  ions, □ and ■ for volume produced  $H^-$  ions with and without Cs.

**Figure 7.** Pressure dependence of hydrogen negative ions obtained by model calculation:  $H^-$  (2) versus gas pressure  $p$  with and without Cs, where  $T_e(1) = 5 \text{ eV}$ ,  $T_e(2) = 1 \text{ eV}$  and  $n_e(1) = 5 \times 10^{12} \text{ cm}^{-3}$ .

**Figure 8.** Estimation of the extracted  $H^-$  ions with Cs: extracted  $H^-$  ions versus  $p$ , corresponding to the results shown in Fig. 7, where solid line shows the previous result and dotted circle shows the present results.

**Figure 9.** Extracted  $H^-$  ions versus  $p$ , corresponding to the results shown in Fig. 7.

## Table captions

**Table 1.** Some plasma parameters obtained by the model calculation when hydrogen gas pressure  $p = 5$  mTorr.

**Table 2.** Numerical results of  $H^-$  transport, where  $p = 5$  mTorr,  $B_0 = 120$  G and  $l_B = 4$  cm.

**Table 3.** Numerical results of  $H^-$  transport, where  $p = 1$  mTorr,  $B_0 = 120$  G and  $l_B = 4$  cm.

**Table 4.** Procedure for estimation of extracted  $H^-$  ions, corresponding to the result shown in Fig. 7.

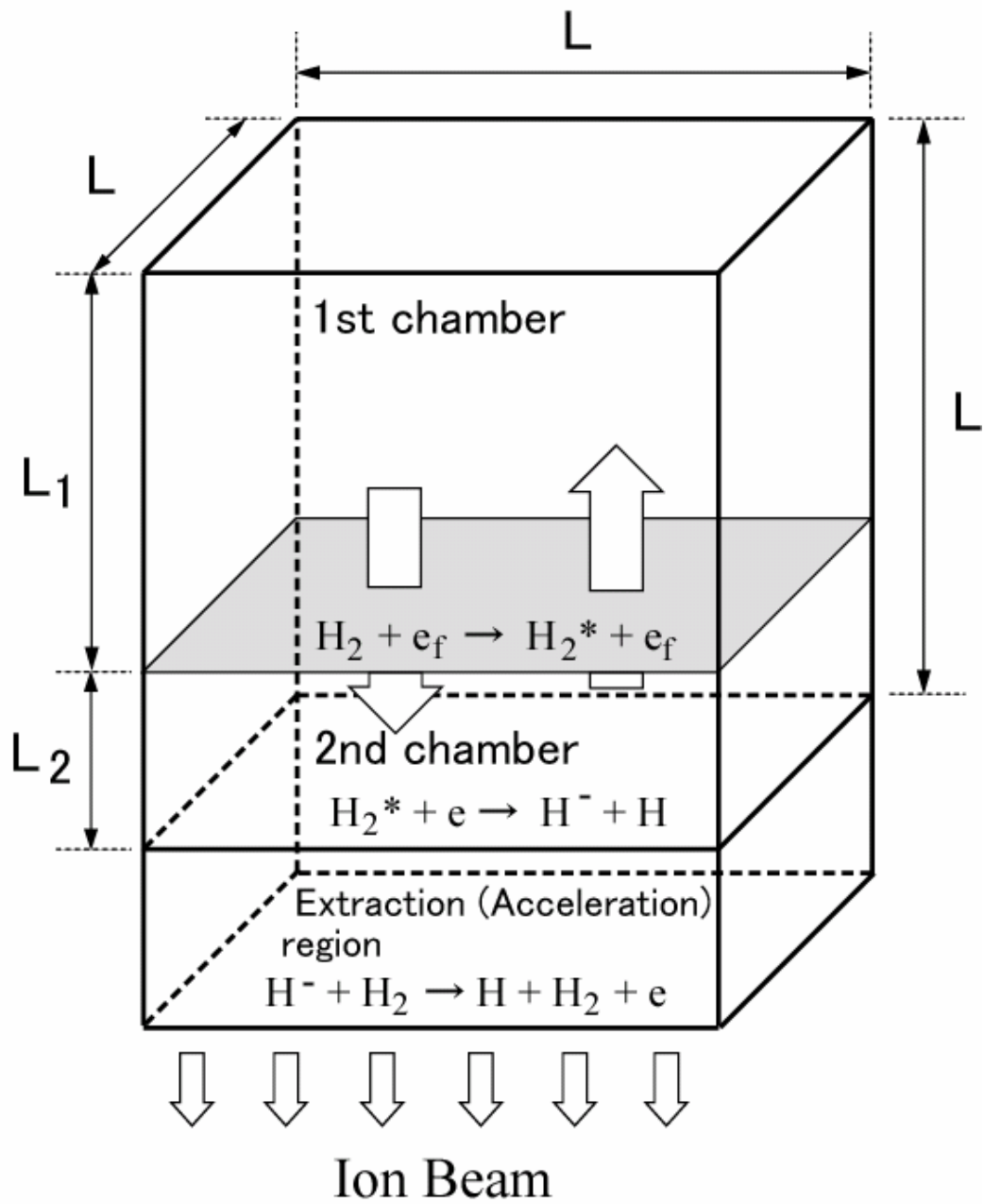


Fig. 1 O.Fukumasa

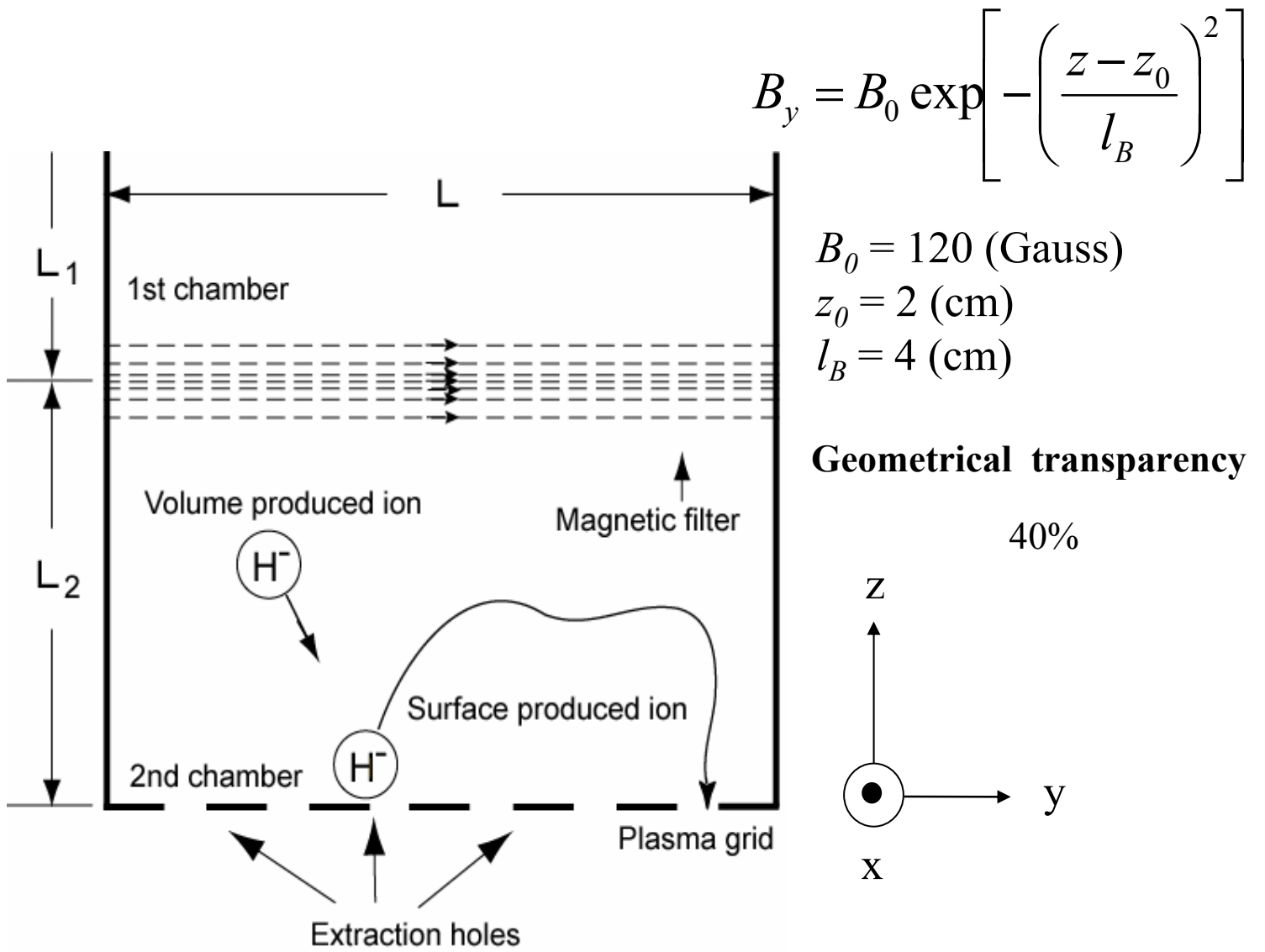


Fig. 2 O.Fukumasa

( a )

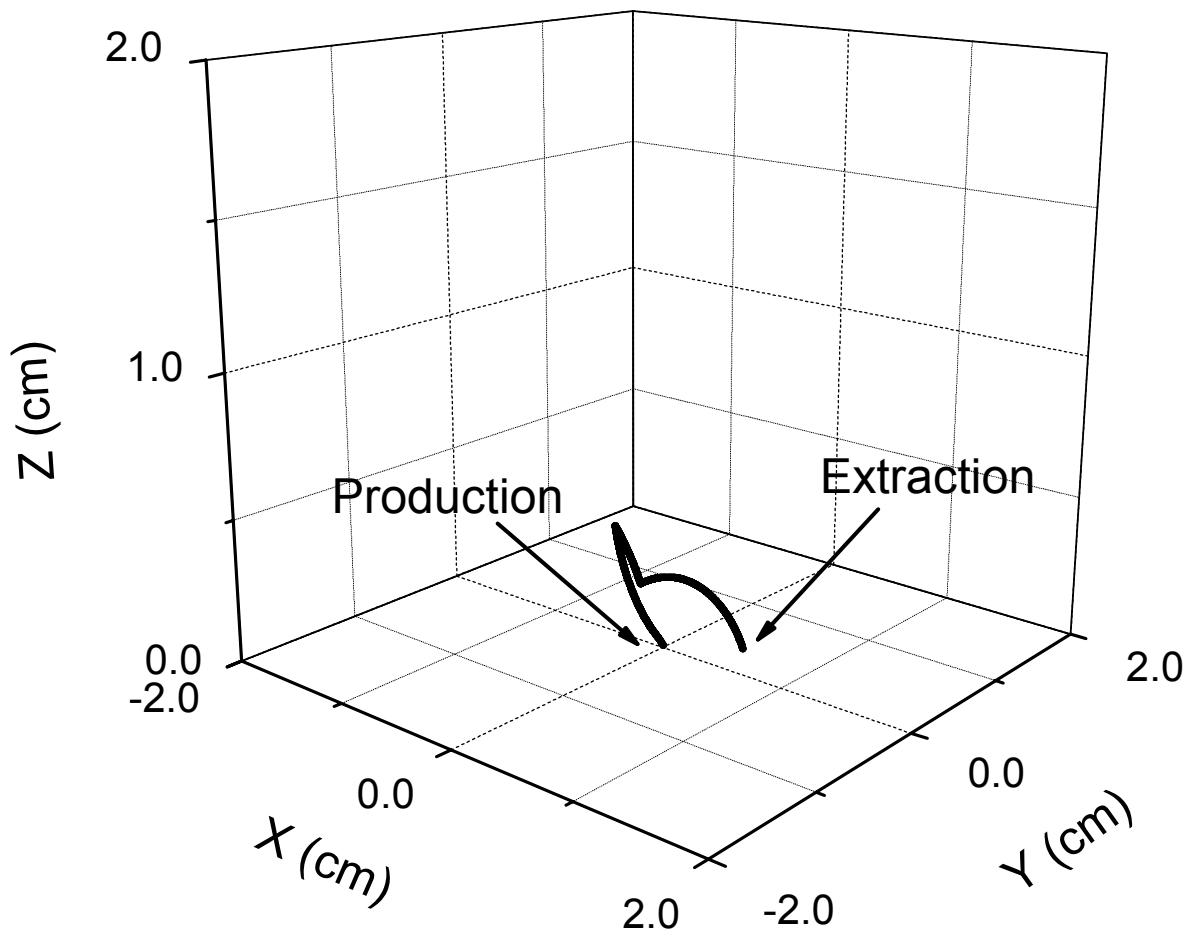


Fig. 3 O.Fukumasa

(b)

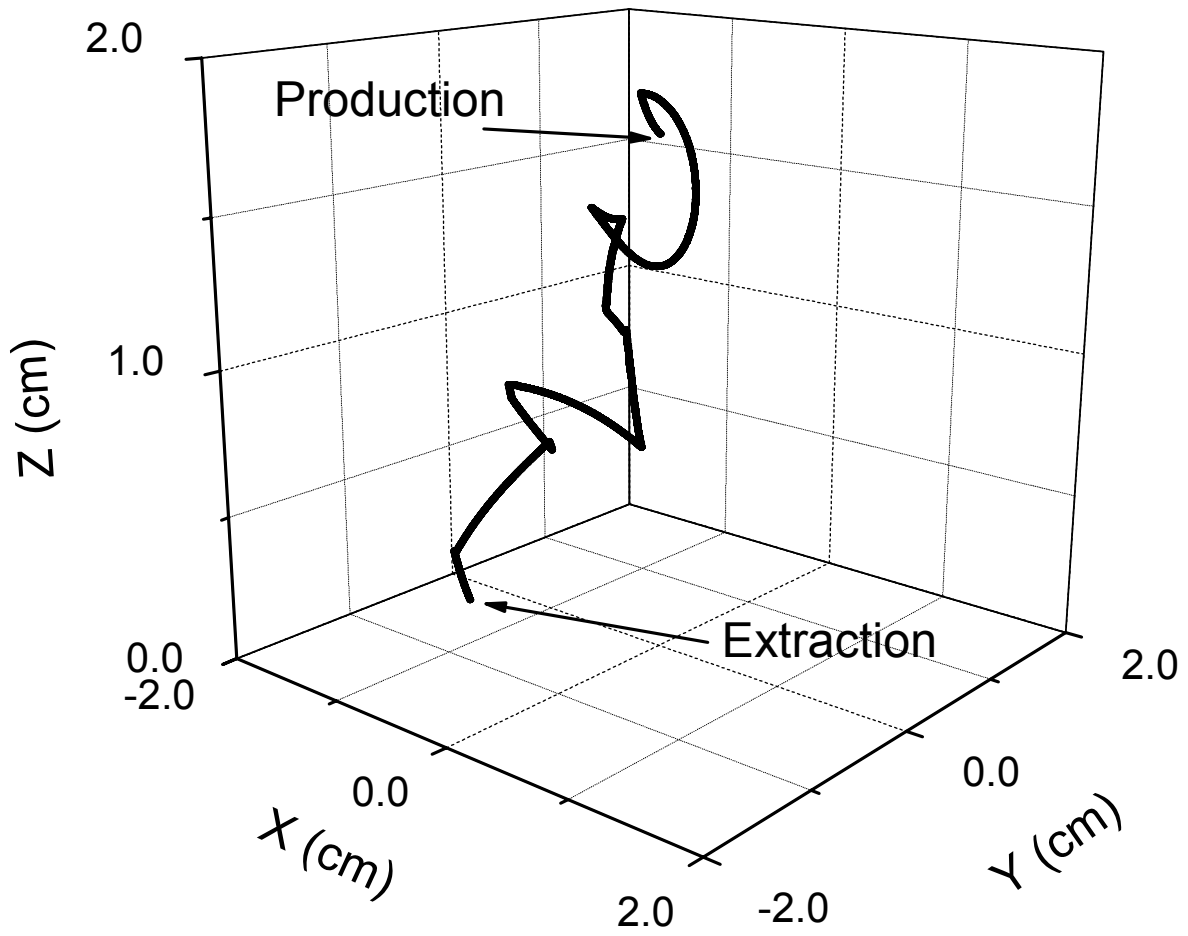


Fig. 3 O.Fukumasa

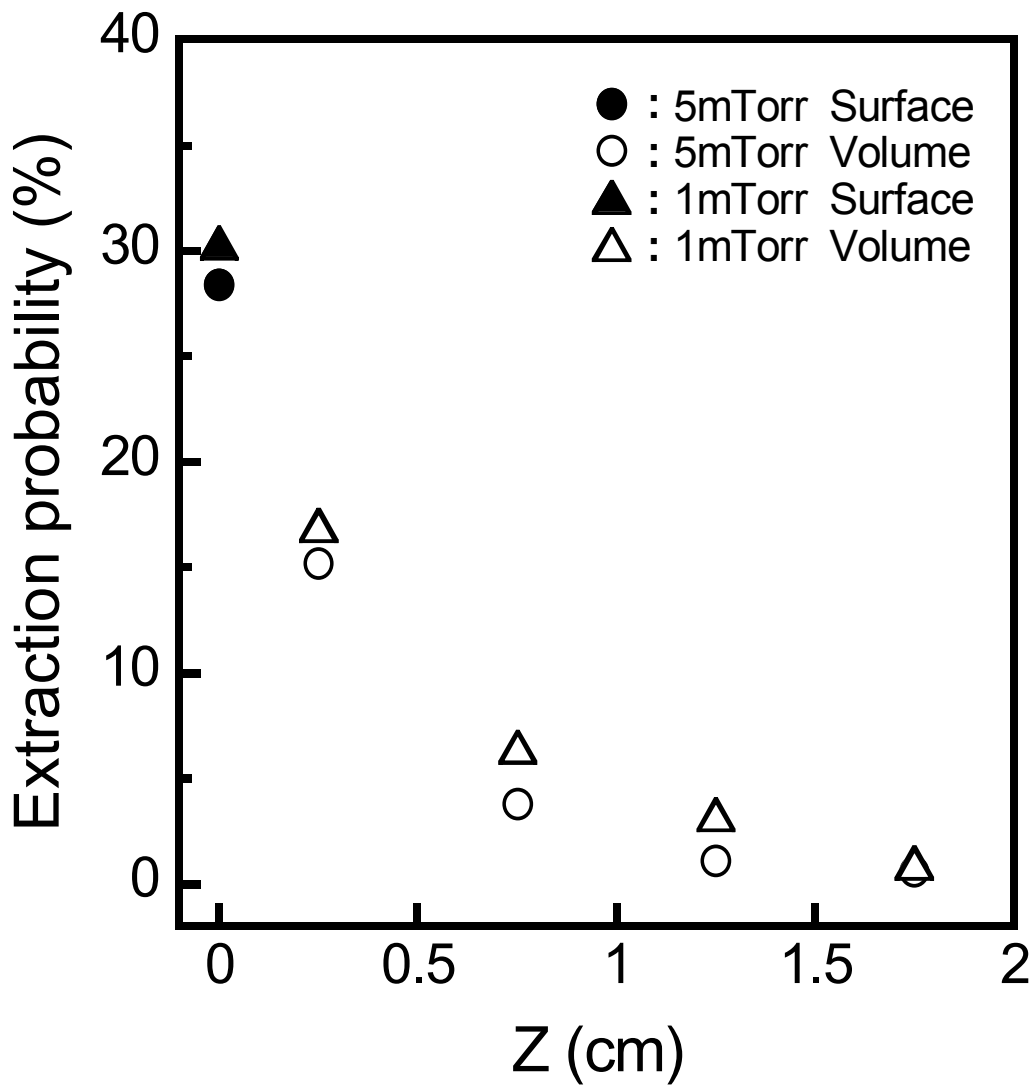


Fig. 4 O.Fukumasa

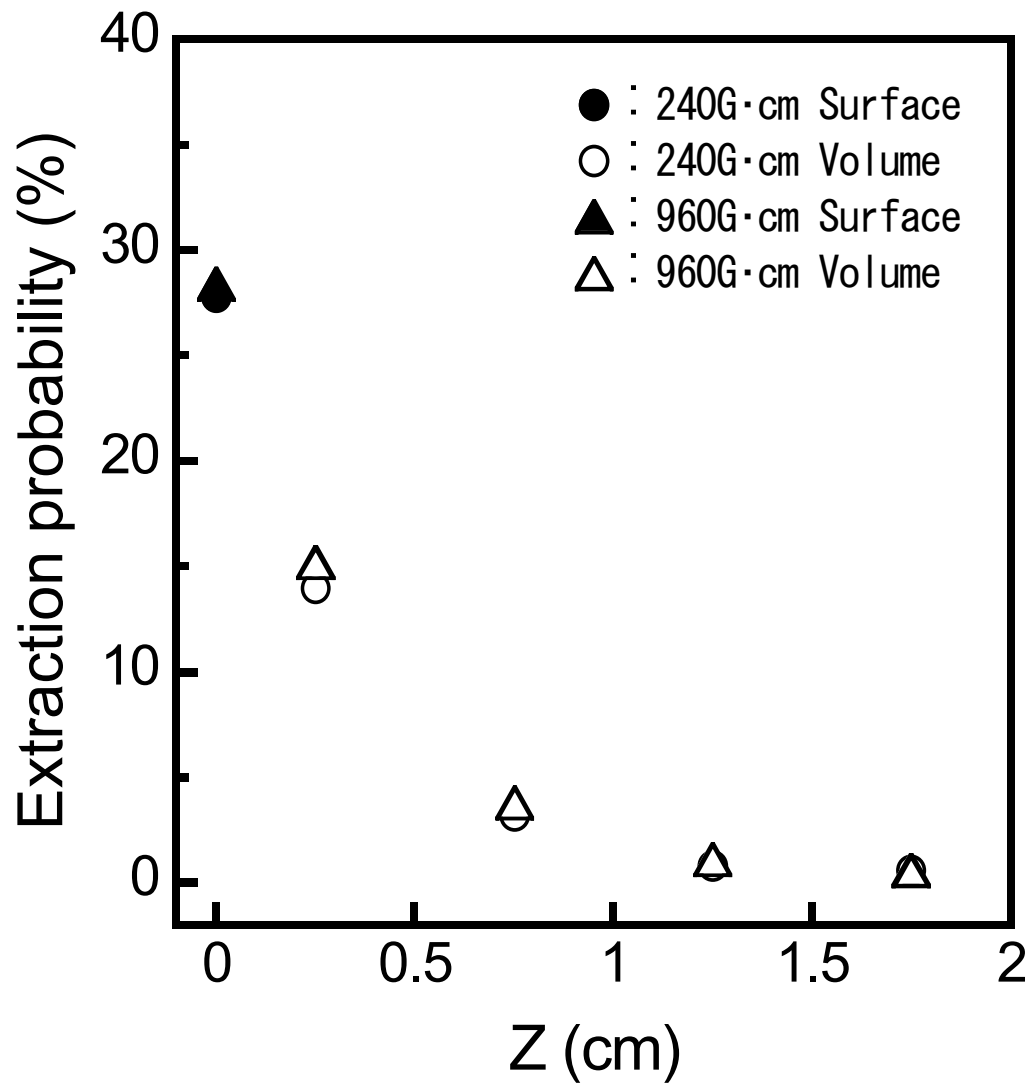


Fig. 5 O.Fukumasa

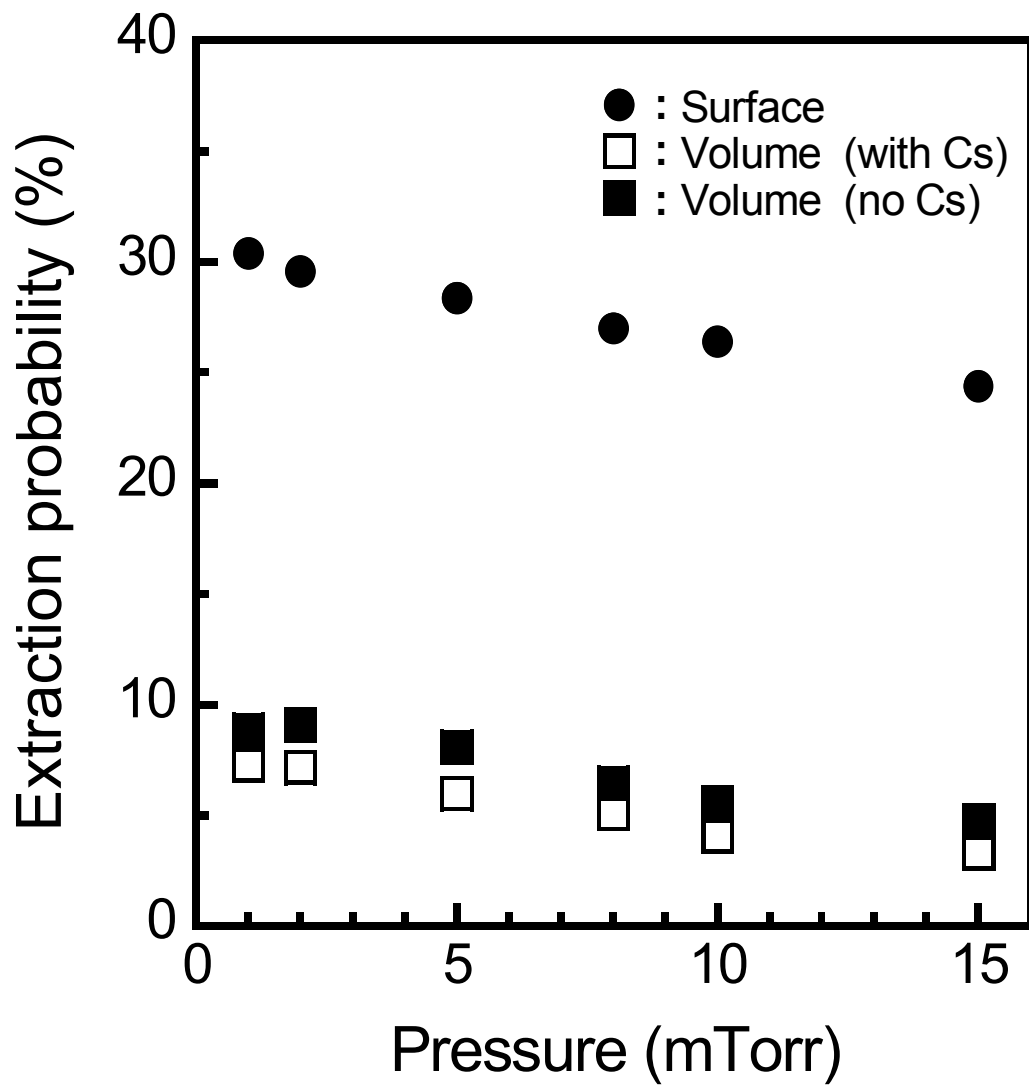


Fig. 6 O.Fukumasa

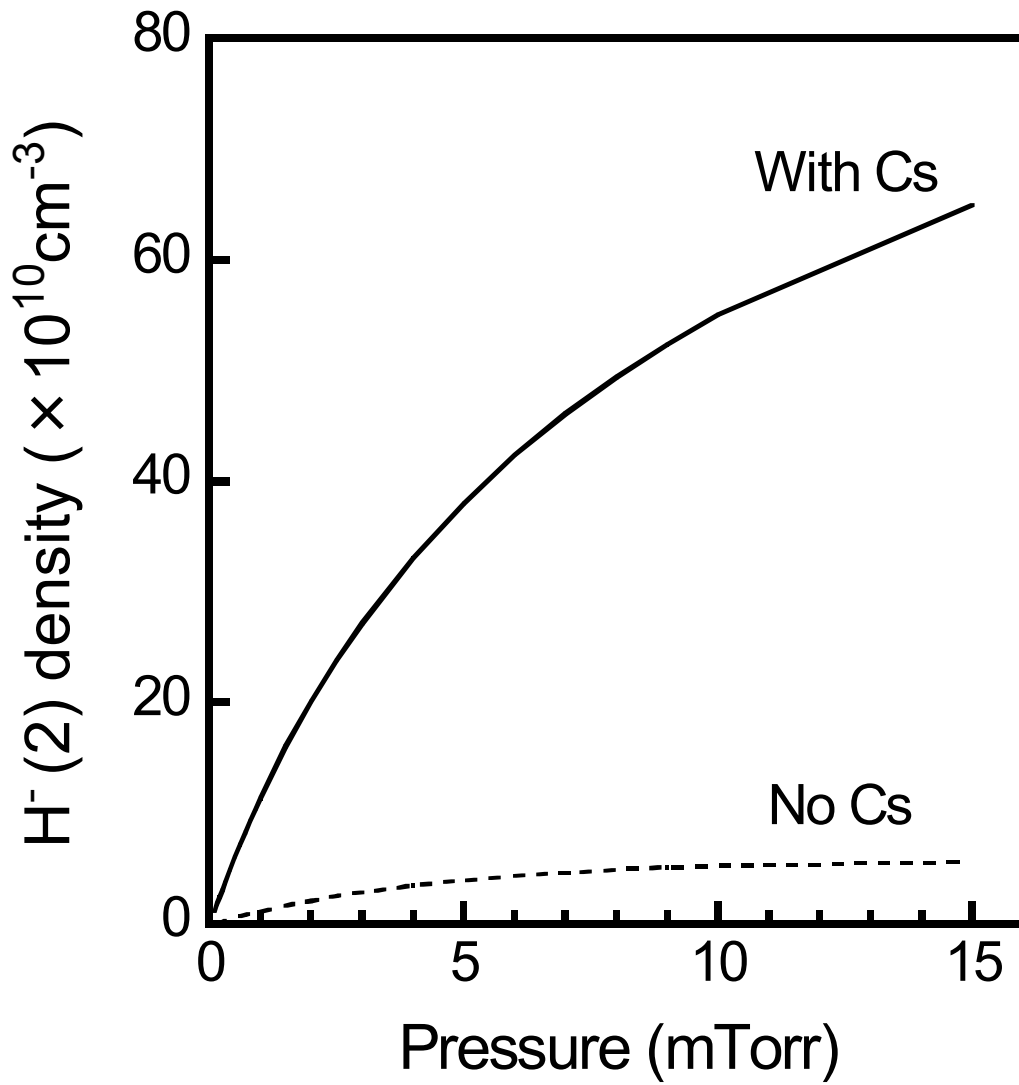


Fig. 7 O.Fukumasa

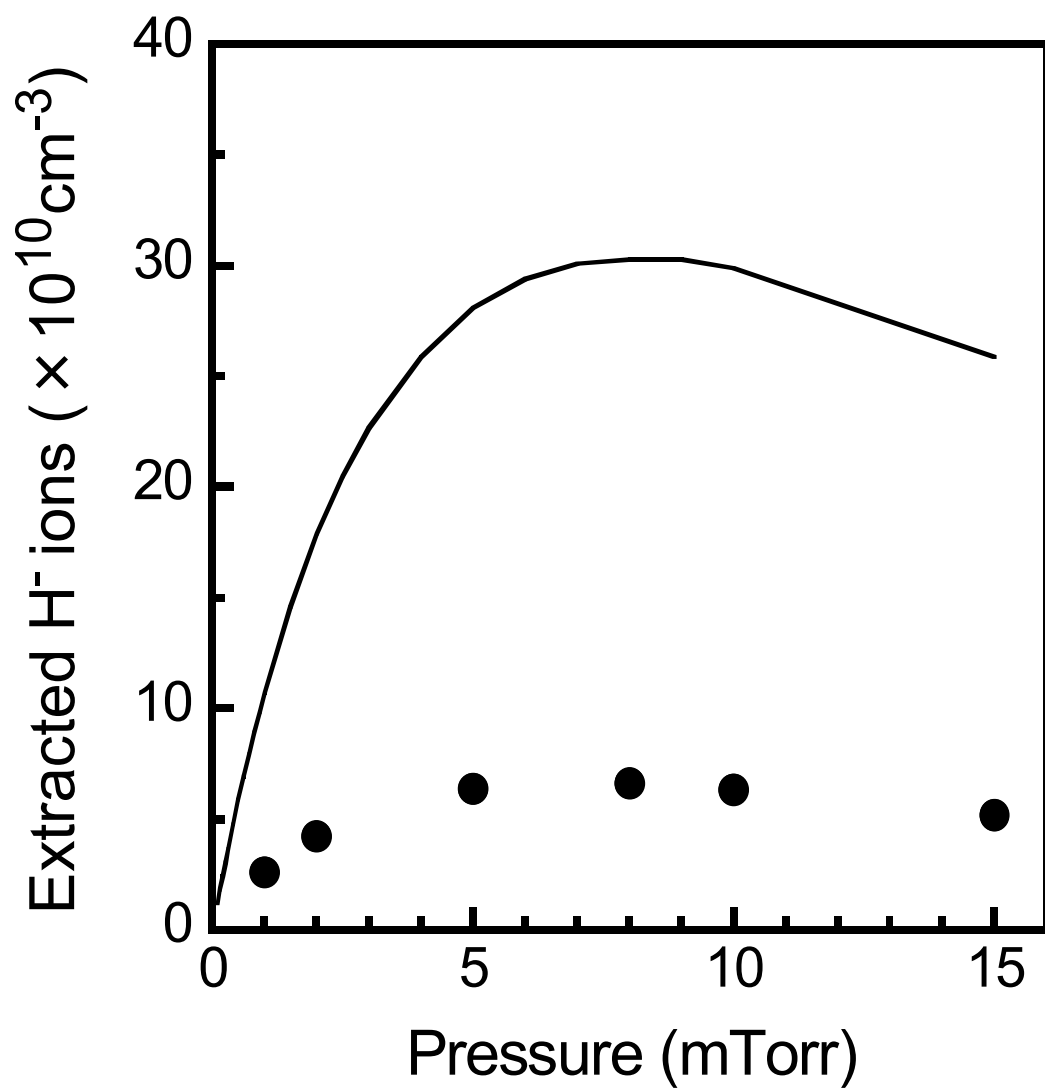


Fig. 8 O.Fukumasa

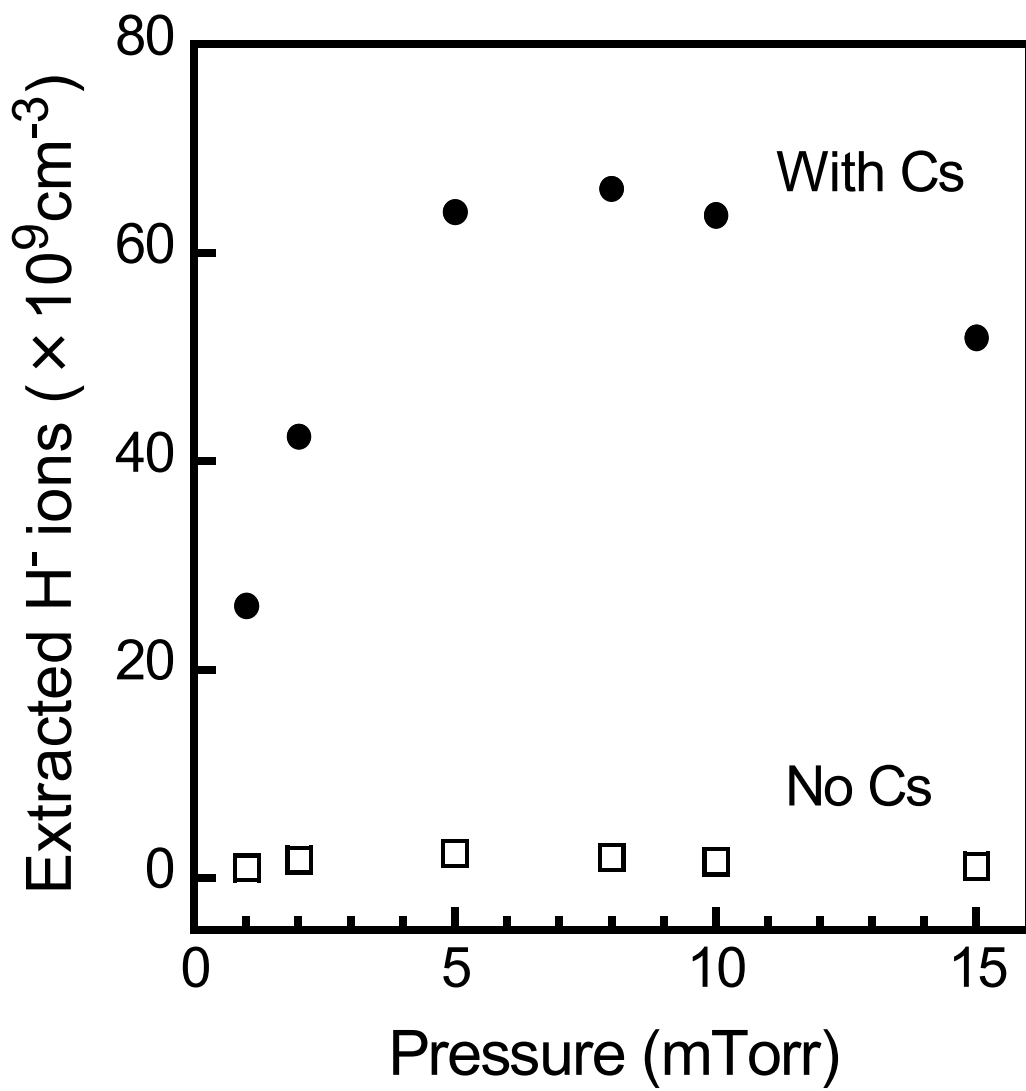


Fig. 9 O.Fukumasa

$n_{H^-}$	H <sup>-</sup> ion density	$3.81 \times 10^{11} \text{ cm}^{-3}$
$n_e$	Electron density	$1.00 \times 10^{12} \text{ cm}^{-3}$
$n_H$	H atom density	$5.22 \times 10^{13} \text{ cm}^{-3}$
$n_{H_2}$	H atom density	$8.31 \times 10^{13} \text{ cm}^{-3}$
$n_{H^+}$	H <sup>+</sup> ion density	$3.73 \times 10^{11} \text{ cm}^{-3}$
$n_{H_2^+}$	H <sup>+</sup> ion density	$2.71 \times 10^{11} \text{ cm}^{-3}$
$n_{H_3^+}$	H <sup>+</sup> ion density	$1.52 \times 10^{11} \text{ cm}^{-3}$
$n_{Cs^+}$	Cs <sup>+</sup> ion density	$5.85 \times 10^{11} \text{ cm}^{-3}$
$n_{Cs}$	Cs atom density	$4.41 \times 10^{12} \text{ cm}^{-3}$
$T_e$	Electron temperature	1.0 eV
$T_H$	H atom temperature	0.5 eV
$T_{H^+}$	H <sup>+</sup> ion temperature	0.5 eV

Table. 1 O.Fukumasa

<b>H<sup>-</sup> ions</b> <b>Collisions</b>		<b>Surface produced H<sup>-</sup> ions</b>	<b>Volume produced H<sup>-</sup> ions</b>			
			<b>Birth point from the PG [cm]</b>			
			<b>0.25</b>	<b>0.75</b>	<b>1.25</b>	<b>1.75</b>
<b>Wall loss</b>		<b>16</b>	<b>31</b>	<b>51</b>	<b>53</b>	<b>57</b>
<b>Collisional destruction</b>	<b>e</b>	<b>13</b>	<b>24</b>	<b>65</b>	<b>127</b>	<b>258</b>
	<b>H<sup>+</sup></b>	<b>33</b>	<b>83</b>	<b>113</b>	<b>127</b>	<b>103</b>
	<b>H<sub>2</sub><sup>+</sup></b>	<b>26</b>	<b>68</b>	<b>87</b>	<b>79</b>	<b>70</b>
	<b>H<sub>3</sub><sup>+</sup></b>	<b>11</b>	<b>31</b>	<b>46</b>	<b>33</b>	<b>33</b>
	<b>H</b>	<b>44</b>	<b>115</b>	<b>165</b>	<b>162</b>	<b>145</b>
	<b>H<sub>2</sub></b>	<b>80</b>	<b>186</b>	<b>242</b>	<b>257</b>	<b>196</b>
	<b>Cs<sup>+</sup></b>	<b>57</b>	<b>55</b>	<b>103</b>	<b>99</b>	<b>97</b>
	<b>Cs</b>	<b>10</b>	<b>28</b>	<b>33</b>	<b>36</b>	<b>27</b>
<b>Total</b>		<b>274</b>	<b>590</b>	<b>854</b>	<b>920</b>	<b>929</b>
<b>Elastic collision</b>	<b>H<sup>+</sup></b>	<b>682</b>	<b>1494</b>	<b>2161</b>	<b>1999</b>	<b>1517</b>
<b>Charge exchange</b>	<b>H</b>	<b>1464</b>	<b>3007</b>	<b>4416</b>	<b>4389</b>	<b>3776</b>
<b>H<sup>-</sup> ions reach the PG</b>		<b>710</b>	<b>379</b>	<b>95</b>	<b>27</b>	<b>14</b>
<b>Average energy of the above H<sup>-</sup> ions [eV]</b>		<b>0.66</b>	<b>0.46</b>	<b>0.42</b>	<b>0.44</b>	<b>0.48</b>
<b>Extraction probability [%]</b>		<b>28.4</b>	<b>15.2</b>	<b>3.8</b>	<b>1.1</b>	<b>0.6</b>

( Mean value 5.2% )

Table. 2 O.Fukumasa

<b>H<sup>-</sup> ions Collisions</b>		<b>Surface produced H<sup>-</sup> ions</b>	<b>Volume produced H<sup>-</sup> ions</b>			
			<b>Birth point from the PG [cm]</b>			
			<b>0.25</b>	<b>0.75</b>	<b>1.25</b>	<b>1.75</b>
<b>Wall loss</b>		<b>29</b>	<b>54</b>	<b>71</b>	<b>77</b>	<b>68</b>
<b>Collisional destruction</b>	<b>e</b>	<b>20</b>	<b>59</b>	<b>117</b>	<b>185</b>	<b>346</b>
	<b>H<sup>+</sup></b>	<b>36</b>	<b>98</b>	<b>130</b>	<b>129</b>	<b>118</b>
	<b>H<sub>2</sub><sup>+</sup></b>	<b>20</b>	<b>41</b>	<b>54</b>	<b>56</b>	<b>55</b>
	<b>H<sub>3</sub><sup>+</sup></b>	<b>1</b>	<b>9</b>	<b>11</b>	<b>11</b>	<b>6</b>
	<b>H</b>	<b>13</b>	<b>54</b>	<b>64</b>	<b>88</b>	<b>80</b>
	<b>H<sub>2</sub></b>	<b>23</b>	<b>63</b>	<b>99</b>	<b>83</b>	<b>56</b>
	<b>Cs<sup>+</sup></b>	<b>88</b>	<b>161</b>	<b>242</b>	<b>230</b>	<b>203</b>
	<b>Cs</b>	<b>10</b>	<b>37</b>	<b>49</b>	<b>59</b>	<b>43</b>
<b>Total</b>		<b>211</b>	<b>522</b>	<b>766</b>	<b>841</b>	<b>907</b>
<b>Elastic collision</b>	<b>H<sup>+</sup></b>	<b>1043</b>	<b>3047</b>	<b>3992</b>	<b>3992</b>	<b>2942</b>
<b>Charge exchange</b>	<b>H</b>	<b>428</b>	<b>1199</b>	<b>1678</b>	<b>1865</b>	<b>2212</b>
<b>H<sup>-</sup> ions reach the PG</b>		<b>760</b>	<b>424</b>	<b>163</b>	<b>82</b>	<b>25</b>
<b>Average energy of the above H<sup>-</sup> ions [eV]</b>		<b>0.69</b>	<b>0.46</b>	<b>0.42</b>	<b>0.44</b>	<b>0.49</b>
<b>Extraction probability [%]</b>		<b>30.4</b>	<b>17.0</b>	<b>6.5</b>	<b>3.3</b>	<b>1.0</b>

( Mean value 7.0% )

Table. 3 O.Fukumasa

		Pressure [mTorr]					
		1	2	5	8	10	15
<b>H<sup>-</sup>(2) ion density</b> [ $\times 10^{10} \text{ cm}^{-3}$ ]		11.4	20.2	38.1	49.5	55.1	65.0
<b>A rate of H<sup>-</sup> formation [%]</b>	<b>SP</b>	73.6	73.4	74.1	74.9	75.5	76.9
	<b>VP</b>	26.4	26.6	25.9	25.1	24.5	23.1
<b>Estimated H<sup>-</sup> ions</b> [ $\times 10^{10} \text{ cm}^{-3}$ ]	<b>SP</b>	8.39	14.8	28.2	37.1	41.6	50.0
	<b>VP</b>	3.01	5.36	9.87	12.4	13.5	15.0
<b>Extraction probability of H<sup>-</sup> ions [%]</b>	<b>SP</b>	30.4	29.6	28.4	27.0	26.4	24.4
	<b>VP</b>	7.3	7.2	6.0	5.1	4.1	3.3
<b>H<sup>-</sup> ions reach the PG</b> [ $\times 10^{10} \text{ cm}^{-3}$ ]	<b>SP</b>	2.55	4.39	8.01	10.0	10.9	12.2
	<b>VP</b>	0.22	0.38	0.59	0.63	0.55	0.49
<b>H<sup>-</sup> ions reach the PG (total)</b> [ $\times 10^{10} \text{ cm}^{-3}$ ]		2.77	4.77	8.60	10.6	11.5	12.7
<b>Survival factor F against the stripping loss [%]</b>		94.2	88.8	74.3	62.2	55.2	40.9
<b>Extracted H<sup>-</sup> ions from the ion source</b> [ $\times 10^{10} \text{ cm}^{-3}$ ]		2.61	4.24	6.39	6.62	6.36	5.19

SP : Surface Production , VP : Volume Production

Table. 4 O.Fukumasa